

Supporting Information:

Phosphonium Salt & $\text{ZnX}_2\text{-PPh}_3$ Integrated Hierarchical POPs: Tailorable Synthesis and Highly Efficient Cooperative Catalysis in CO_2 Utilization

Cunyao Li^{1, 3†}, Wenlong Wang^{1†}, Li Yan^{1*}, Yuqing Wang^{1, 3}, Miao Jiang¹, and Yunjie Ding^{1,2*}

¹ Dalian National Laboratory for Clean Energy. Dalian, 116023, PR China.

*E-mail: dyj@dicp.ac.cn and yanli@dicp.ac.cn.

² State Key Laboratory of Catalysis, Dalian Institute of Chemical Physics, Chinese Academy of Sciences.

³ University of Chinese Academy of Sciences. Beijing, 10039, PR China

†These authors contributed equally to this paper.

Table of contents:

| | |
|--|-----------|
| 1. Supplementary figures | 2 |
| 2. Analytical data for compounds $3\text{vP}^+\text{Br}^-$ and $3\text{vP}^+\text{I}^-$ | 9 |
| 3. NMR spectra of $3\text{vP}^+\text{Br}^-$ and $3\text{vP}^+\text{I}^-$ | 10 |

1. Supplementary figures

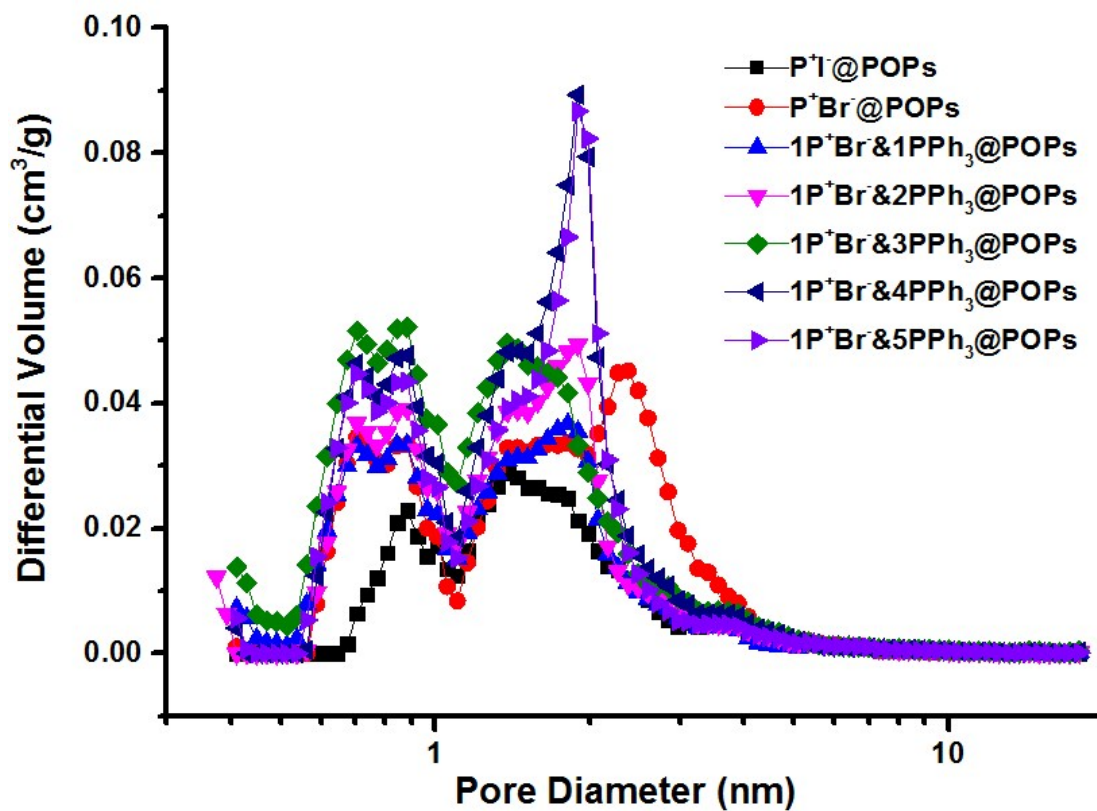


Figure S1. Pore sizes distributions of the afforded polymers.

Figure S1 showed the pore size distribution curves of the afforded porous organic polymers calculated from non-local density functional theory (NLDFT). The pore sizes were mainly distributed at 0.70, 0.85, 1.45, 2-18 nm respectively.

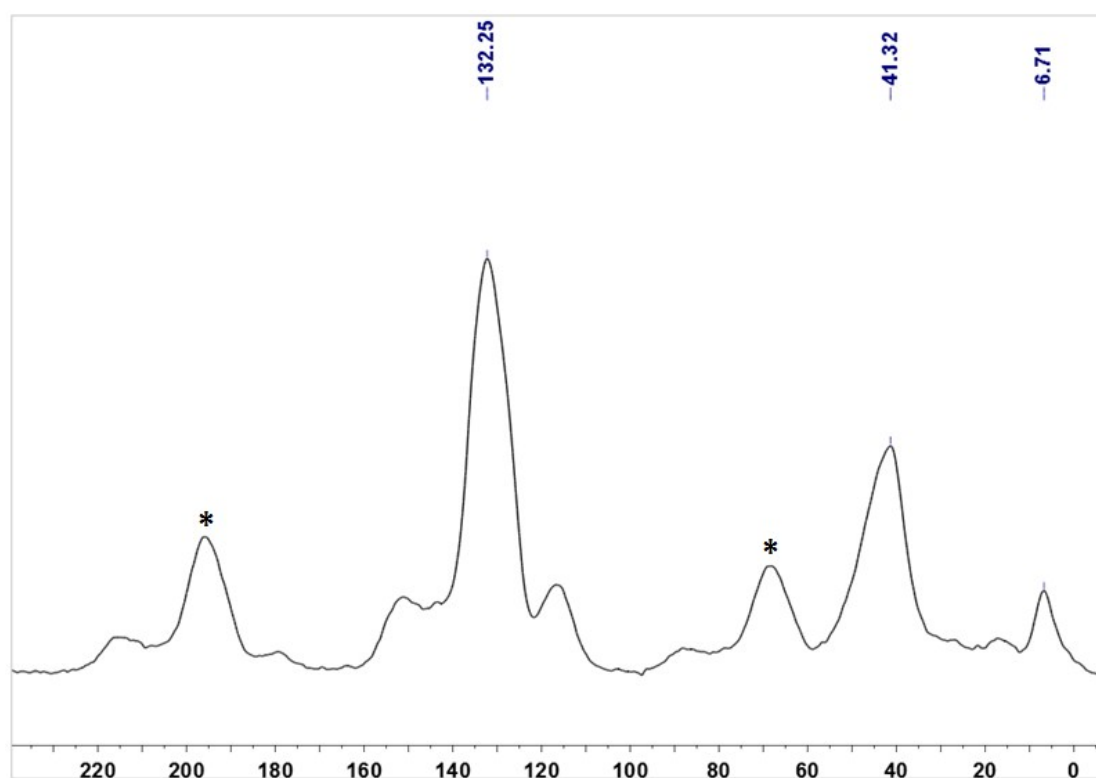


Figure S2. ^{13}C MAS NMR spectrum of $1\text{P}^+\text{Br}^-1\text{PPh}_3@POPs$.

The peaks at * are side bands. Compared with the NMR spectra of the monomers 3vPPh_3 and $3\text{vP}^+\text{Br}^-$ (see below NMR spectra), the additional peaks at 41.3 ppm was attributed to the polymerized vinyl groups. The signals ranged from 120 to 150 ppm could be attributed to the aromatic carbons.

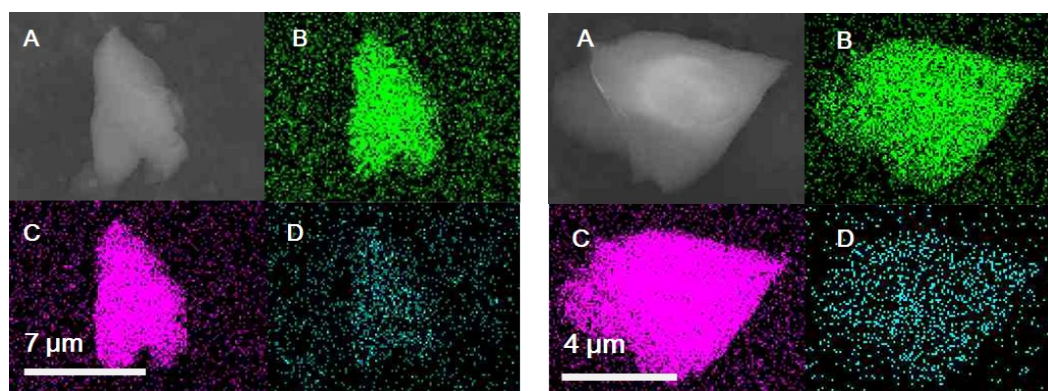


Figure S3. Elemental distribution in fresh $1\text{P}^+\text{Br}^-1\text{PPh}_3@POPs$ (left) and used $1\text{P}^+\text{Br}^-1\text{PPh}_3@POPs$ (right) determined by SEM-EDS mapping, (A) SEM images, (B) Phosphorus, (C) Bromine and (D) Zinc.

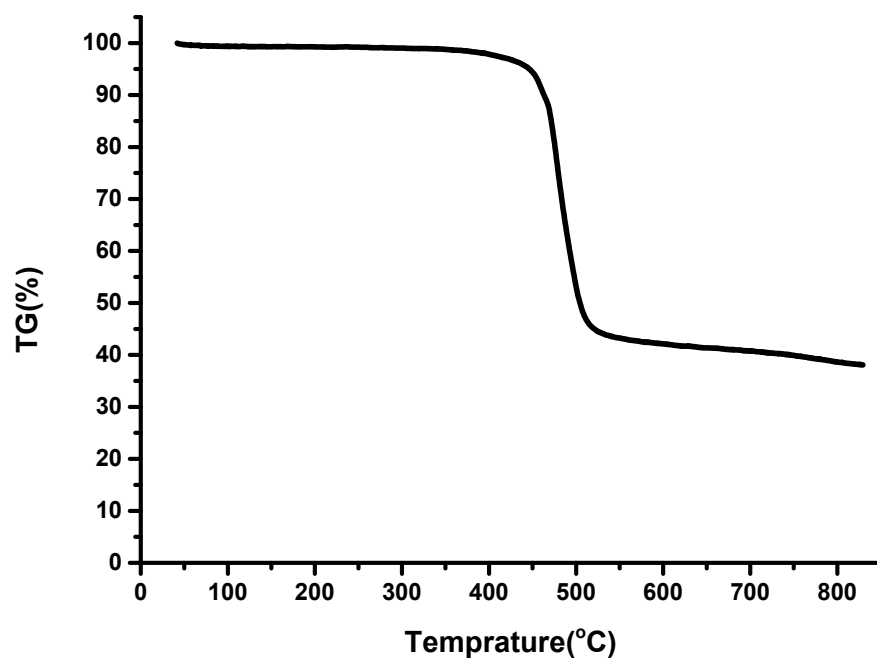


Figure S4. TG curve of the afforded $1P^+Br^-1PPh_3@POPs$ polymer.

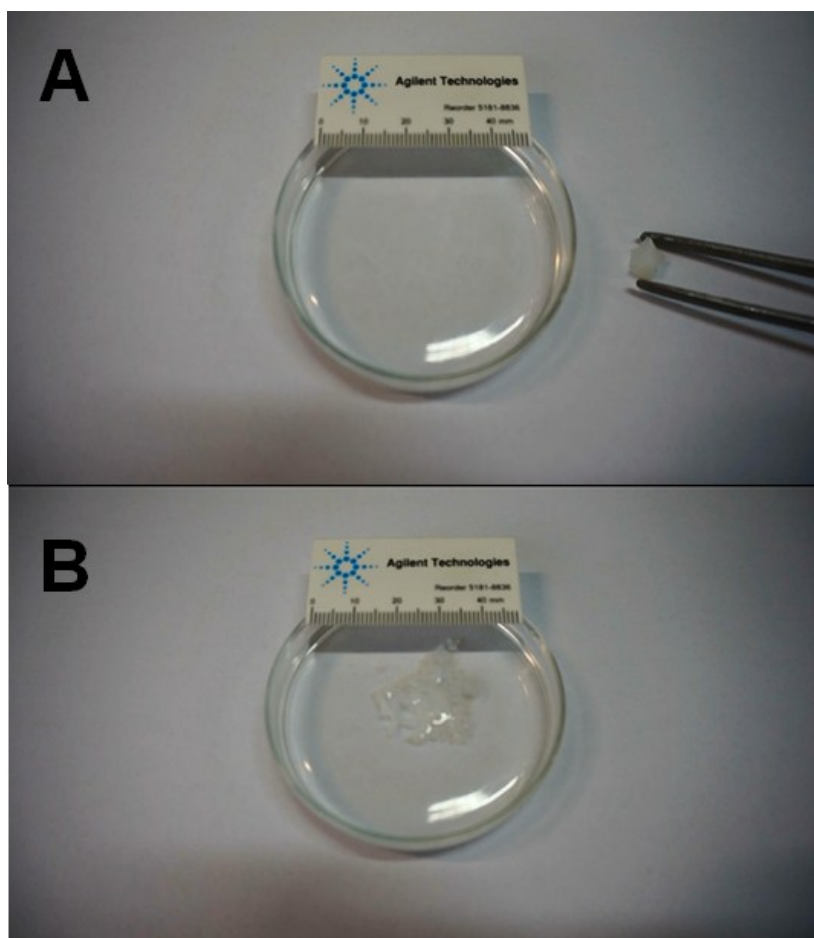


Figure S5. Photograph of the $1P^+Br^-$ & $1PPh_3@POPs$ in dry state (A) and in THF solution (B). The $1P^+Br^-$ & $1PPh_3@POPs$ could swell in other solution such as DMF, toluene, ethanol and propylene oxide as well, indicating the well-swelling property of the polymer.

The isosteric heats of adsorption (Q_{st}) of $1P^+Br^-1PPh_3@POPs$ and $P^+Br^-@POPs$ polymers were calculated according to Clausius-Clapeyron equation:

$$\ln\left(\frac{P_1}{P_2}\right) = Q_{st} \times \frac{T_2 - T_1}{R \times T_1 \times T_2}$$

where Q_{st} is the isosteric heats of adsorption, T_i represents a temperature at which an isotherm i is measured, P_i represents a pressure at which a specific equilibrium adsorption amount is reached at T_i , R is gas constant ($8.314 \text{ J K}^{-1} \text{ mol}^{-1}$).

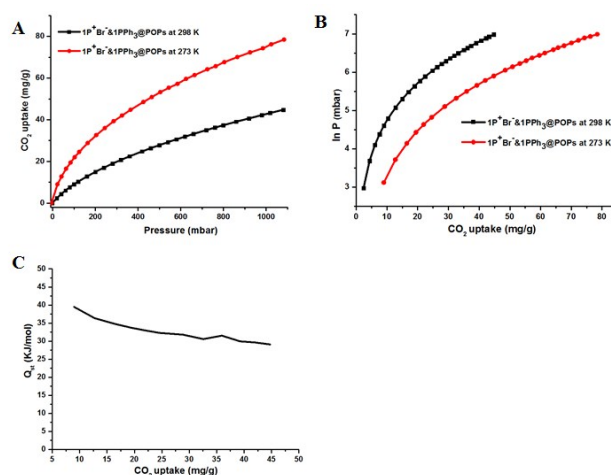


Figure S6. (A) The CO₂ isotherms of $1P^+Br^-1PPh_3@POPs$ polymer at 298 K and 273 K; (B) The plots of lnP vs. CO₂ uptake of $1P^+Br^-1PPh_3@POPs$ polymer at 298 K and 273 K calculated from the data in (A); (C) The plot of Q_{st} vs. CO₂ uptake calculated from the data in (B) based on Clausius-Clapeyron equation.

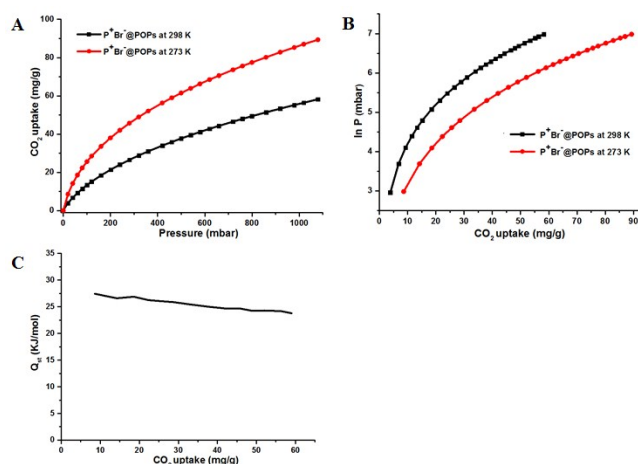


Figure S7. (A) The CO₂ isotherms of $P^+Br^-@POPs$ polymer at 298 K and 273 K; (B) The plots of lnP vs. CO₂ uptake of $P^+Br^-@POPs$ polymer at 298 K and 273 K calculated from the data in (A); (C) The plot of Q_{st} vs. CO₂ uptake calculated from the data in (B) based on Clausius-Clapeyron equation.

As shown in Figure S6 (C), the Q_{st} of prepared $1P^+Br^- \& 1PPh_3@POPs$ polymer decreased slowly from 40 KJ/mol to 30 KJ/mol with the increasing of CO_2 uptake from 10 mg/g to 45 mg/g. Comparatively, the Q_{st} of $P^+Br^-@POPs$ decreased from 27 KJ/mol slowly to 23 KJ/mol with the increasing of CO_2 uptake from 10 mg/g to 60 mg/g (Figure 7 C). The Q_{st} data of hybrid $1P^+Br^- \& 1PPh_3@POPs$ polymer was higher than $P^+Br^-@POPs$ under the same CO_2 uptake, showing the CO_2 -philic properties of the extra doped PPh_3 units in the polymer.

To test the porosity texture of the POPs and loading catalytic pormoters, $P^+Br^-ZnBr_2-1PPh_3@POPs$ was chosen as a representative catalyst and the N_2 sorption isotherm of $P^+Br^-ZnBr_2-1PPh_3@POPs$ catalyst was attached below(Figure S8). The BET surface area was $458.2\text{ m}^2/\text{g}$ while the total pore volume was $0.435\text{ cm}^3/\text{g}$. And the catalyst also showed the hierarchical pore size distribution. After loading Zn, the POPs maintained its microporosity.

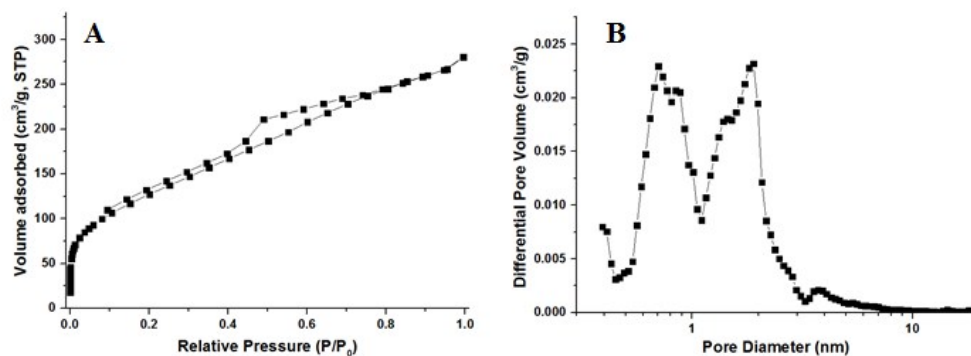
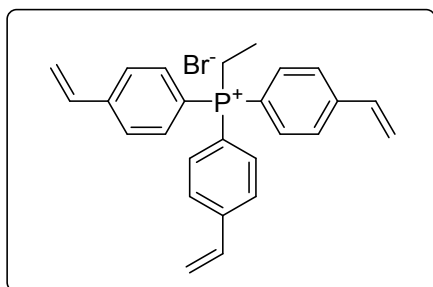
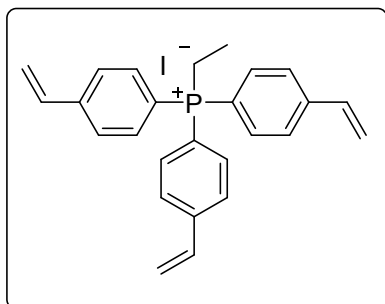


Figure S8. (A) Nitrogen sorption isotherm and (B) Pore sizes distribution of $P^+Br^-ZnBr_2-1PPh_3@POPs$ catalyst.

2. Analytical data for compounds $3vP^+Br^-$ and $3vP^+I^-$



¹H NMR (400 MHz, CDCl₃) δ 1.26-1.38(m, 3H), 3.58-3.78 (m, 2H), 5.35-5.50 (m, 3H), 5.81-5.96 (m, 3H), 6.60-6.78 (m, 3H), 7.54-7.98 (m, 12H); **¹³C NMR** (100 MHz, CDCl₃) δ 6.7, 6.8, 17.0, 17.5, 116.1, 117.0, 119.3, 127.9, 128.0, 133.8, 133.9, 134.9, 143.9, 144.0; **³¹P NMR** (161.8 MHz, CDCl₃) δ 25.3;



¹H NMR (400 MHz, CDCl₃) δ 1.26-1.40(m, 3H), 3.54-3.68 (m, 2H), 5.48 (dd, 3H, $J_1 = 10.7$ Hz, $J_2 = 3.0$ Hz), 5.93 (d, 3H, $J = 17.0$ Hz), 6.65-6.80 (m, 3H), 7.62-7.98 (m, 12H); **¹³C NMR** (100 MHz, CDCl₃) δ 6.7, 6.7, 17.3, 17.8, 115.8, 116.7, 119.3, 127.8, 128.0, 133.7, 133.8, 134.7, 143.9, 144.0; **³¹P NMR** (161.8 MHz, CDCl₃) δ 25.2;

3. NMR spectra of 3vP⁺Br⁻ and 3vP⁺I⁻

